ACS OMEGA

http://pubs.acs.org/journal/acsodf

Article

Electrocatalytic CO_2 Reduction by [$Re(CO)_3Cl$(3-(pyridin-2-yl)-5-phenyl-1,2,4-triazole)] and [$Re(CO)_3Cl$(3-(2-pyridyl)-1,2,4-triazole)]

Phuong N. Nguyen, Thi-Bich-Ngoc Dao, Trang T. Tran, Ngoc-Anh T. Tran, Tu A. Nguyen, Thao-Dang L. Phan, Loc P. Nguyen, Vinh Q. Dang, Tuan M. Nguyen,* and Nam N. Dang

Cite This: *ACS Omega* 2022, 7, 34089−34097

Read Online

ACCESS | Metrics & More | Article Recommendations | Supporting Information

ABSTRACT: The exploration of novel electrocatalysts for CO_2 reduction is necessary to overcome global warming and the depletion of fossil fuels. In the current study, the electrocatalytic CO_2 reduction of [$Re(CO)_3Cl(N\text{-}N)$], where *N*-*N* represents 3-(2-pyridyl)-1,2,4-triazole (Hpy), 3-(pyridin-2-yl)-5-phenyl-l,2,4-triazole (Hph), and 2,2′-bipyridine-4,4′ dicarboxylic acidic (bpy-COOH) ligands, was investigated. In CO_2-saturated electrolytes, cyclic voltammograms showed an enhancement of the current at the second reduction wave for all complexes. In the presence of triethanolamine (TEOA), the currents of Re(Hpy), Re(Hph), and Re(bpy-COOH) enhanced significantly by approximately 4-, 2-, and 5-fold at peak potentials of −1.60, −150, and −1.69 $V_{Ag/Ag+}$, respectively (in comparison to without TEOA). The reduction potential of Re(Hph) was less negative than those of Re(Hpy) and Re(COOH), which was suggested to cause its least efficiency for CO_2 reduction. Chronoamperometry measurements showed the stability of the cathodic current at the second reduction wave for at least 300 s, and Re(COOH) was the most stable in the CO_2-catalyzed reduction. The appearance and disappearance of the absorption band in the UV/vis spectra indicated the reaction of the catalyst with molecular CO_2 and its conversion to new species, which were proposed to be Re-**DMF**$^+$ and Re-**TEOA** and were supposed to react with CO_2 molecules. The CO_2 molecules were claimed to be captured and inserted into the oxygen bond of Re-**TEOA**, resulting in the enhancement of the CO_2 reduction efficiency. The results indicate a new way of using these complexes in electrocatalytic CO_2 reduction.

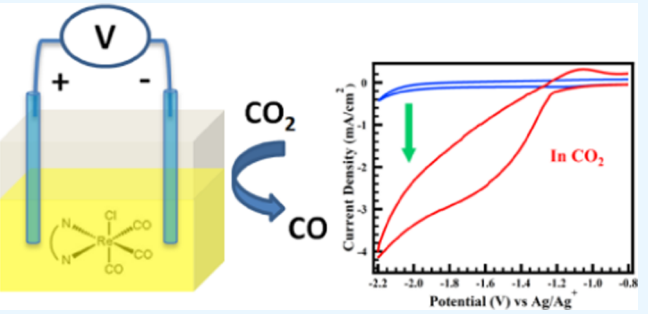

1. INTRODUCTION

Carbon dioxide is identified as one of the main gases causing global warming. In the twenty-first century, carbon dioxide emission increased rapidly from 270 ppm (parts per million) in the early 1800s to 418 ppm in January 2022,[1] resulting in a high concentration of CO_2 in the atmosphere. CO_2 is released through human activities, heavy industrial activities, traffic, burning of fossil fuels, deforestation, and respiration. Therefore, using CO_2 as a resource for the generation of fuels and chemical energy has attracted great attention. Converting CO_2 to fuels can contribute to the efforts toward solving two serious problems, including the depletion of fossil resources and global warming. Among CO_2 reduction methods, electrocatalysis is known as the most promising approach to CO_2 conversion because the potential of CO_2 reduction is effortless to achieve and it can be carried out at room temperature with high selectivity.[2−4] The CO_2 reduction reaction by homogeneous catalysts based on metal complexes commonly involves multiple numbers of electrons and protons, and the potentials required to reduce CO_2 are −0.52, −0.48, −0.38, and −0.24 V for 2, 4, 6, and 8 electron reduction, respectively.[5] Although electrocatalytic conversion of CO_2 has been studied for decades, the exploration of a novel catalytic design and finding appropriate electrocatalysts that work at low overpotential and with high selectivity for CO_2 reduction still remain topics of interest.[6−8] The electrocatalytic reduction of CO_2 has been widely investigated, including metal-2,2-bipyridyl-based compounds,[9−15] metal carbonyl compounds, 13 porphyrinoid compounds,[16] and metal carbene compounds.[17,18] The amount of complexes containing pyridyl-triazole or its derivatives based on iridium(III), rhodium(III), ruthenium(II), and osmium(II) has been characterized[19−23] structurally, photophysically, and electrochemically; however, the electrocatalytic reduction of CO_2 based on these complexes has not been extensively explored.

Homogeneous electrocatalysts are preferred for investigations over heterogeneous electrocatalysts because of their

Received: May 31, 2022
Accepted: September 5, 2022
Published: September 14, 2022

https://doi.org/10.1021/acsomega.2c03278
ACS Omega 2022, 7, 34089−34097

Scheme 1. Structural Representation of the Ligands and Rhenium Complexes Synthesized and Investigated in this Study

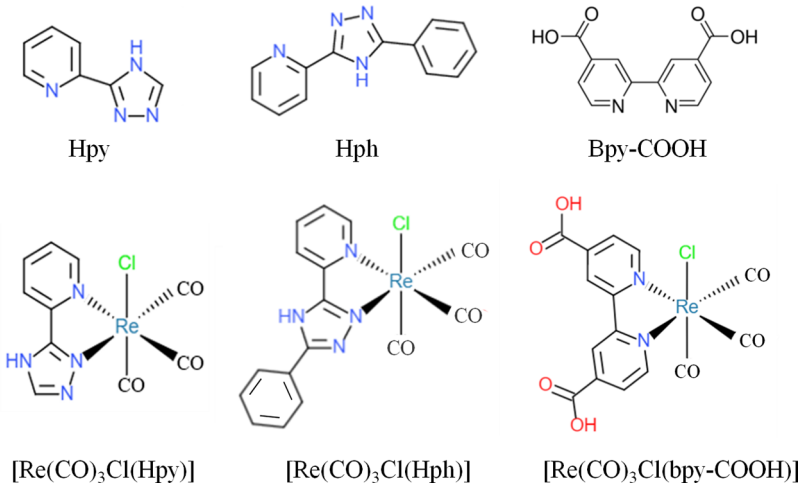

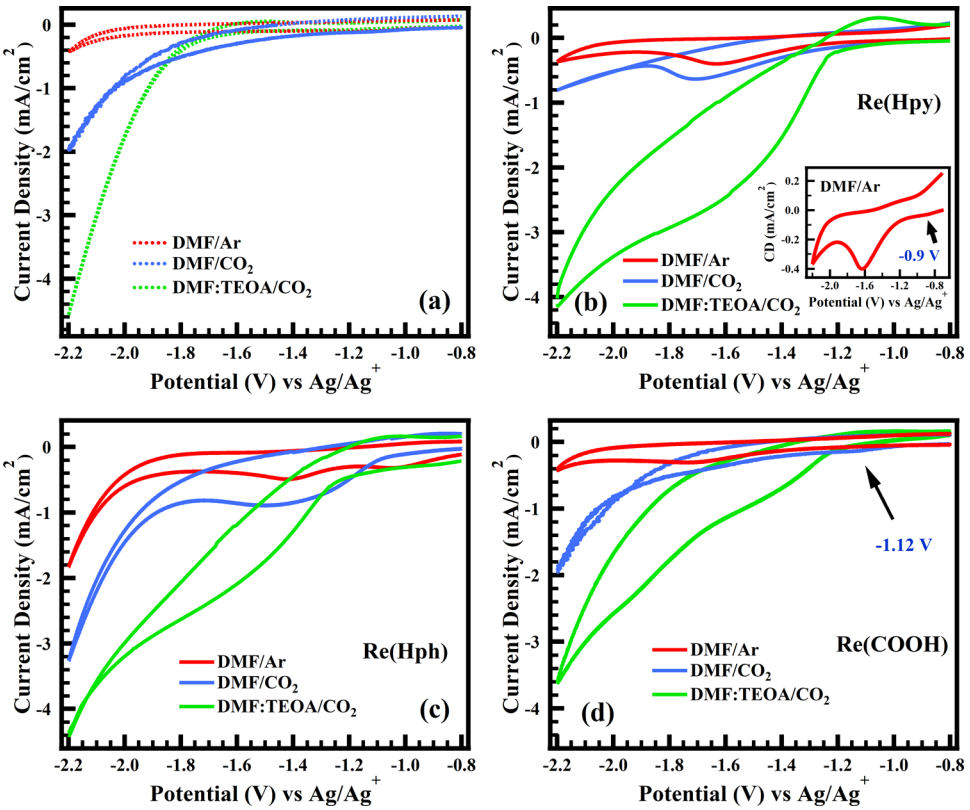

Figure 1. Cyclic voltammograms of the (a) blank solvent DMF under Ar (dotted red line) and CO_2 (dotted blue line) and DMF:TEOA under CO_2 (dotted green line) and of (b) Re(Hpy), (c) Re(Hph), and (d) Re(COOH) in the DMF solvent under Ar and CO_2 and in a DMF:TEOA mixed solution under CO_2. The red and blue lines represent the CV of each complex in the DMF solvent under Ar and CO_2, respectively. The green line shows the CV of the complex in a DMF:TEOA solution under CO_2. The CV of Re(Hpy) in a DMF solvent under Ar is shown in the inset in (b).

simple structures and properties.[23,24] Therefore, homogeneous electrocatalysts serve as a key to understand crucial features for an efficient electrocatalytic CO_2 reduction reaction. The electrochemical properties of homogeneous complexes (d_6 metal centers such as Re(I), Ru(II), etc.) based on pyridyl−triazole ligands are controlled by the σ-donor and π-acceptor properties of the ligands in the coordination sphere.[19] In particular, pyridyl−triazole ligands exhibited stronger σ-donor and weaker π-acceptor properties than 2,2′-bipyridyl and 2,2′-bipyridyl derivatives.[25,26] The ligands influence the redox potential of these complexes; a strong σ-donor donates electron density to the metal center, leading to lower oxidation potentials and more negative reduction potentials. The electrochemical CO_2 reduction of rhenium complexes based on 2-pyridyl-1,2,3-triazole ligands was reported as a new CO_2 reduction catalysis.[27,28] The series of Re(I) complexes based on 4-(2-pyridyl)-1,2,3-triazole and 1-(2-pyridyl)-1,2,3-triazole diimine ligands catalyzed the electroreduction of CO_2 using water as a proton source; meanwhile, the electrocatalytic CO_2 reduction of complexes based on 3-(2-pyridyl)-1,2,4-triazole

https://doi.org/10.1021/acsomega.2c03278
ACS Omega 2022, 7, 34089−34097

Table 1. Reduction Potentials and Current Densities of the Complexes at the Corresponding Reduction Potentials

			cathodic current density (mA/cm^2)			
complex	Re^I	Re^{II}	(1st)	(2nd)	solvent	atmosphere
Re(Hpy)	−0.90	−1.64	0.03	0.4	DMF	Ar
	−0.90	−1.69	0.05	0.63	DMF	CO_2
		−1.60		2.46	DMF:TEOA	CO_2
Re(Hph)	−1.02	−1.41	0.32	0.48	DMF	Ar
	−1.02	−1.41	0.12	0.87	DMF	CO_2
	−1.02	−1.50	0.32	1.72	DMF:TEOA	CO_2
Re(COOH)	−1.12	−1.69	0.07	0.30	DMF	Ar
	−1.12	−1.69	0.13	0.42	DMF	CO_2
	−1.45	−1.91	0.82	2.27	DMF:TEOA	CO_2

Scheme 2. Formation of New Species and the CO_2 Insertion Process

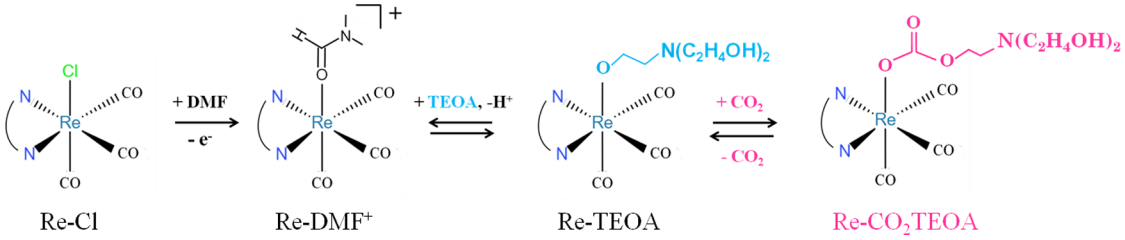

and 3-(pyridin-2-yl)-5-phenyl-l,2,4-triazole ligands have not been investigated yet.

Re complexes based on pyridin−triazole ligands have been well-known to possess interesting optical properties,[29,30] have a low negative reduction potential that can be applied for electrocatalytic CO_2 reduction,[27] and be easy to prepare in good yield.[26] To explore new features of other classes of Re diimine complexes (a typical class of Re diimine complex constitutes Re complexes based on polypyridine), [Re(CO)$_3$Cl(Hpy)], [Re(CO)$_3$Cl(Hph)], and [Re(CO)$_3$Cl(bpy-COOH)] (bpy-COOH is a derivative of the bpy ligand) have been recommended for the first time and characterized as catalysts for CO_2 electroreduction. 3-(2-Pyridyl)-1,2,4-triazole and 3-(pyridin-2-yl)-5-phenyl-l,2,4-triazole ligands and their corresponding Re complexes, shown in Scheme 1, were synthesized with good yield and characterized by proton nuclear magnetic resonance (1H NMR), electrospray ionization mass spectroscopy (ESI-MS), and Fourier transform infrared spectroscopy (FTIR). The electrocatalytic CO_2 reduction of these complexes was evaluated via cyclic voltammetry (CV) in the absence and presence of CO_2 gas and with/without a proton source. Chronoamperometry (CA) analysis was also applied to determine the stability and CO_2 reduction current, which is used to calculate the power generated at the applied potential. In addition, UV/vis measurement was used to trace the changes in the catalysts before and after the CO_2 reduction reaction.

2. RESULTS AND DISCUSSION

2.1. Electrochemical Studies under an Inert Atmosphere. Electrochemical behaviors of Re(Hpy), Re(Hph), and Re(COOH) were studied in a DMF solution with Ar-saturated electrolytes in the potential range of −0.8 to −2.2 V (Figure 1). The cyclic voltammogram of the blank electrolytes under an Ar atmosphere is shown in Figure 1a (dotted red line). In the Ar-saturated solution, three complexes show two reduction waves. The first one-electron reductions of Re(Hpy), Re(Hph), and Re(COOH) appear at −0.9 (see the inset in Figure 1b), −1.02, and −1.12 V, followed by the second irreversible one-electron reductions at −1.64, −1.41, and −1.69 V, respectively. The first reduction was attributed to a ligand-based reduction. The irreversible second reduction wave was attributed to the generation of the two-electron-reduced species. The reduction potentials of Re(Hpy) and Re(Hph) are less negative than that of Re(COOH), which indicates that pyridyl−triazole ligands are stronger acceptors than 2,2′-bipyridine-4,4′ dicarboxylic acid. The lower reduction potential of Re(Hph) than that of Re(Hpy) was in agreement with the results of Brennan.[34] The reduction peak position and current density corresponding to each reduction peak are summarized in Table 1.

2.2. Electrochemical Studies under a CO_2 Atmosphere. To study the electrochemical CO_2 reduction of Re(Hpy), Re(Hph), and Re(COOH), CV measurements of these complexes were performed in a DMF solution and a DMF:TEOA mixed solution in CO_2-saturated electrolytes, as shown in Figure 1. In the CO_2-saturated DMF solution, the addition of CO_2 shifted the irreversible second reduction wave to −1.69 V (about 30 mV) for Re(Hpy). In the case of Re(Hph) and Re(COOH), the shift of the reduction wave was not observed, but the reduction waves were widened (Figure 1b−d). The peak position and current density of the first reduction wave were not affected by CO_2 gas. The cathodic current densities of the three complexes increased, which clearly indicates that the three complexes are active toward CO_2 reduction. Re(Hpy), Re(Hph), and Re(COOH) show current enhancements from 0.4 to 0.63 mA/cm^2 at −1.64 V, 0.48 to 0.87 mA/cm^2 at −1.41 V, 0.30 to 0.42 mA/cm^2 at −1.69 V, respectively. At the second reduction wave, [Re(CO)$_3$Cl(*N*-*N*)] (Re−Cl) is supposed to be converted[10,13,35] to [Re(CO)$_3$(DMF)(*N*-*N*)]$^+$ (Re-DMF$^+$) and CO_2 is captured and inserted on Re-DMF$^+$.

2.3. Electrochemical Studies in a CO_2-Saturated DMF:TEOA Mixed Solution. TEOA had a significant effect on the peak shape, peak position, and current intensity. Re(Hpy) and Re(Hph) showed a large reduction wave from

https://doi.org/10.1021/acsomega.2c03278
ACS Omega 2022, 7, 34089−34097

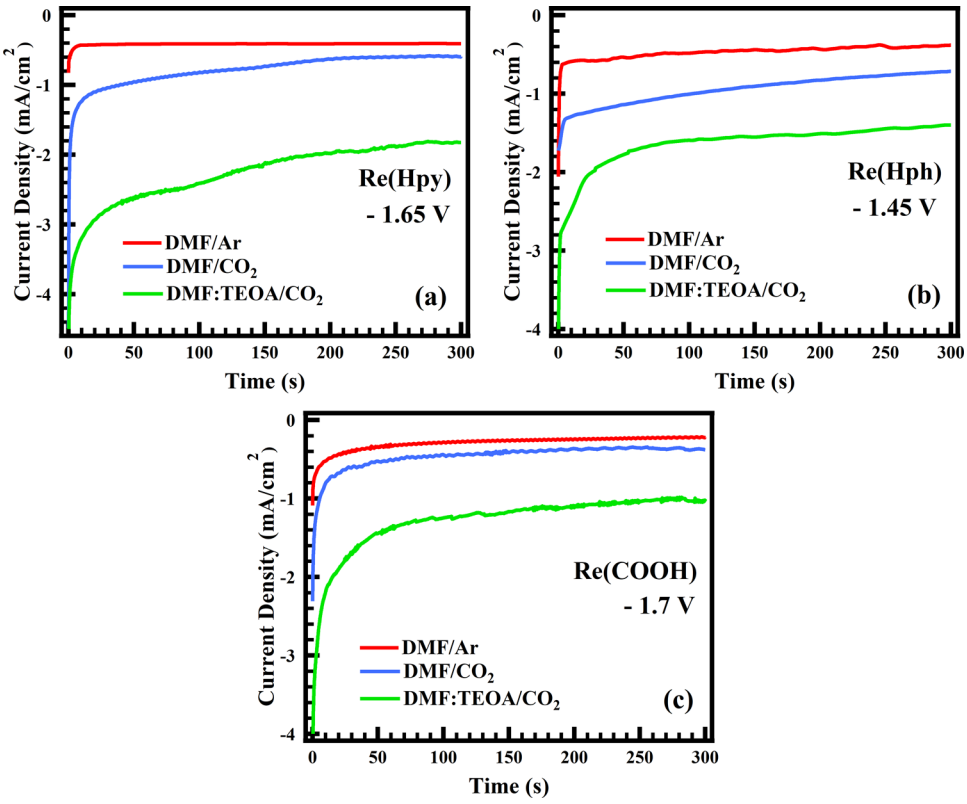

Figure 2. Chronoamperometry analyses of (a) Re(Hpy), (b) Re(Hph), and (c) Re(COOH) in Ar- and CO_2-saturated electrolytes at applied voltages of −1.65, −1.45, and −1.7 V, respectively.

−1.3 to −1.9 V, and Re(COOH) displayed two irreversible reduction waves at −1.45 and −1.91 V. The large reduction waves started after the first reduction wave, which indicated that the reaction with CO_2 took place immediately after the one-electron reduction. The reduction waves that shifted to lower potential and broadened are suggested to the formation of both species of (Re-DMF$^+$), [Re(CO)$_3${OC$_2$H$_4$N-(C$_2$H$_4$OH)$_2$(*N*-*N*)}] ([Re(CO)$_3$(TEOA)(*N*-*N*)]-(Re-TEOA)), and the insertion of CO_2 into the oxygen bond of (Re-TEOA) during the reaction (as shown in Scheme 2).[10,36,37]

The current densities of Re(Hpy), Re(Hph), and Re(COOH) with TEOA increased by approximately 4-, 2-, and 5-fold in comparison to that without TEOA, respectively (Table 1). The enhancement is less significant in Re(Hph) (0.48 to 1.72 mA/cm^2, increased 3.58 times), Re(Hpy) shows a higher enhancement under CO_2 (0.40 to 2.46 72 mA/cm^2, increased approximately 6.15 times), and Re(COOH) shows the highest enhancement (0.30 to 2.27 mA/cm^2, increased 7.57 times). The current enhancement clearly shows that the CO_2 reduction reaction is accelerated under the effect of TEOA. It also showed that Re-TEOA had a higher ability[35] to capture and insert CO_2 than Re-DMF$^+$. Figure 3a displays a comparison of the current densities of the three complexes under different conditions. In the CO_2 reaction involving two-electron reduction, the generated products could be suggested as CO and H_2, and which is in agreement with the CO_2 reduction path with suitable reduction potentials of the developed Re complexes ($CO_2 + 2H^+ + 2e^- \rightarrow CO + H_2O$ at −0.52 V vs SHE at pH = 7).

A chronoamperometry analysis was carried out to investigate the stability and current generation by the CO_2 reduction reactions of Re(Hpy), Re(Hph), and Re(COOH) in Ar- and CO_2-saturated electrolytes at −1.65, −1.45, and −1.7 V, respectively (Figure 2). The measurement time was set at 300 s. The CA curves show good stability of Re(Hpy), Re(Hph), and Re(COOH) for at least 300 ms, and the CO_2 reduction activity of these complexes reduced significantly after 300 s in the CO_2 atmosphere; this decrease is suggested to be because of the decrease in CO_2 concentration in the solution with time. In the Ar atmosphere, the current densities in the three complexes are relatively stable due to the lack of chemical reactions. The average current densities of Re(Hpy), Re(Hph), and Re(COOH) measured in the Ar-saturated DMF solution at their corresponding applied voltages are 0.40, 0.45, and 0.26 mA/cm^2, respectively. In the CO_2-saturated DMF solution, the chronoamperometric data showed that the CO_2 reduction current generated by Re(COOH) was the most stable. Re(Hpy) displayed a relatively low current density after 150 s but was quite stable from 150 to 180 s. Meanwhile, the current density of Re(Hph) decreased immediately after 5 s from 1.47 to 0.71 mA/cm^2. In the presence of TEOA, CA data of all complexes showed high current generation; the current densities generated by Re(Hpy), Re(Hph), and Re(COOH) increased 3.05 (from 0.60 to 1.82 mA/cm^2), 1.96 (from 0.72 to 1.40 mA/cm^2), and 2.75 (from 0.37 to 1.03 mA/cm^2) times, respectively. Based on the current generation, it can be claimed that Re(Hpy) shows high efficiency for CO_2 reduction and Re(Hph) is less efficient than the other two complexes. However, a rapid decrease in the current density after 100 s likely shows that Re(Hpy) is the least stable catalyst for CO_2 reduction. In the common behavior, in the first 20 s, the currents of all complexes decrease drastically, which can be

https://doi.org/10.1021/acsomega.2c03278
ACS Omega 2022, 7, 34089−34097

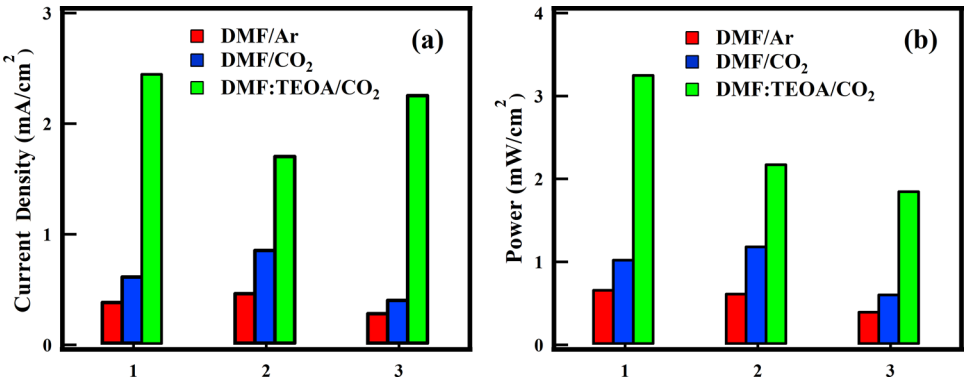

Figure 3. (a) Current density and (b) power in the Ar- and CO_2-saturated electrolytes of Re(Hpy) (1), Re(Hph) (2), and Re(COOH) (3) at the second reduction peak listed in Table 1. The maximum power generation values of (1), (2), and (3) at the applied voltage are shown in Figure 2.

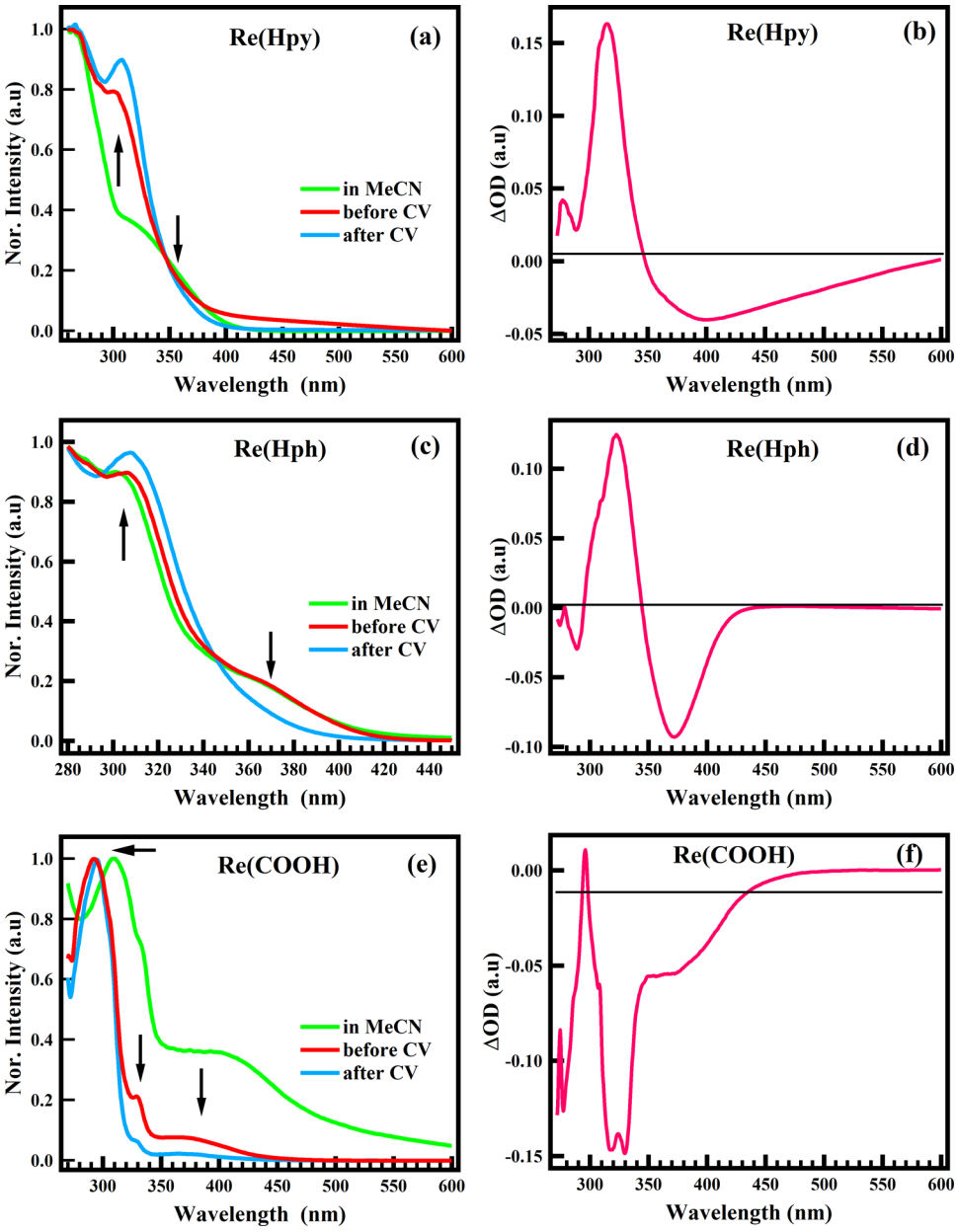

Figure 4. UV/vis spectra of (a) Re(Hpy), (c) Re(Hph), and (e) Re(COOH) in MeCN (light green) and in the DMF:TEOA mixed solution before (red) and after CV measurements (sky blue). The difference in optical densities between UV/Vis spectra obtained after and before CV measurements of (b) Re(Hpy), (d) Re(Hph), and (f) Re(COOH).

https://doi.org/10.1021/acsomega.2c03278
ACS Omega 2022, 7, 34089−34097

explained by the decrease in CO_2 concentration in the solution due to the reaction of CO_2 with the solute.

Figure 3 presents the current density obtained from CV measurements and the power density calculated from the average current (from CA data shown in Figure 2) and the corresponding applied voltage. Figure 3a shows a comparison of the current densities obtained in CV measurements; their values are slightly different from CA data, resulting in the power density. The power density shows the most difference in the CO_2-saturated DMF:TEOA mixed solution. Re(Hpy) shows the highest current, power density, and current enhancement, but Re(COOH) shows the lowest power density although it has the highest applied voltage (Figure 3b). The highest enhancement was observed in Re(Hpy) (approximately 3 times) and the lowest was in Re(Hph) (approximately 1.8 times) because a lower reduction potential[35] could cause the lowest catalytic activity of Re(Hph).

To understand how the catalysts react with molecular CO_2, UV/vis absorption was used to investigate the change in the solution before/after the CV study. UV/vis analysis and the different optical densities are presented in Figure 4. The absorptions of the three complexes in MeCN are shown to compare with those in a DMF:TEOA mixed solution.

2.4. UV/Vis Absorption before CV Measurement. T here was a significant difference in the UV/vis absorptions of these complexes between MeCN and DMF:TEOA solutions. The difference in optical density (DOD) between the UV/vis absorption in MeCN and that in DMF:TEOA solution indicated the formation of new species and the disappearance of the original species. Generally, the DOD allowed us to identify the transformation of the complex in the solution. In Figure 4a, there was a sharp absorption band at 265 nm and a broad absorption from 300 to 400 nm (in MeCN). Changes in absorption were observed at 304 nm and over a wide range from 380 to 560 nm, which indicated the formation of new species absorbing in this range of wavelengths. The negative value of DOD at 360 nm indicates the transformation of the original complex to a species that absorbs at 304 and 402 nm (see SI, Figure S5a). The UV/vis spectrum of Re(Hph) showed that the absorption peak shifted to lower wavelengths when the solution was changed (Figure 4b). This shift resulted in a new sharp absorption peak appearing at 320 nm and the disappearance of an absorption band from 390 to 540 nm (see SI, Figure S5b). Similarly, a change in UV/vis spectra was also observed in Re(COOH), including the shift of the intense absorption peak at 290 nm and the disappearance of a part of the broad absorption from 350 to 450 nm (Figure 4e), which caused the loss of the broad absorption band from 300 to 600 nm. The appearance of a new species was observed at 288 nm with a relatively low intensity (see SI, Figure S5c). The UV/vis spectra in MeCN were measured immediately after the solution was mixed; hence, the ligand Cl could not dissociate and was substituted by MeCN, forming MeCN-coordinated complexes $[Re(CO)_3(MeCN)(N\text{-}N)]$.[38] In addition, the Cl ligand coordinated with the complex was difficult to dissociate, but the complexes were converted into new species, which could be proposed[22] to be Re-DMF$^+$ and Re-TEOA. The underlying mechanism has not been clearly understood yet.

2.5. UV/Vis Absorption after CV Measurement under a CO_2 Atmosphere. The DOD between UV/vis absorptions in the DMF:TEOA solution before and after CV measurement is shown in Figure 4b,d,f. The UV/vis spectra of Re(Hpy) and Re(Hph) (sky blue color in Figure 4a,c) displayed a similar trend, with one positive and one negative absorption peak. However, only one negative absorption band appeared in the DOD of Re(COOH) from 297 to 473 nm. During the CV measurement, the catalysts were undergoing a chemical reaction, and thus, the absorption of the solution after the CV measurement changed. The changes observed in the DOD spectra demonstrate that the catalysts react with CO_2, resulting in the formation of new species. In Figure 4b,d, the peak area of the positive absorption is approximately equal to that of the negative absorption, which indicates that a chemical reaction occurred and the catalysts were converted to other complexes. The conversion is suggested to result from the insertion of CO_2 molecules into the oxygen bond[10,35,39] in Re-TEOA, as shown in Scheme 2.

3. CONCLUSIONS

The electrocatalytic CO_2 reductions of Re(Hpy), Re(Hph), and Re(COOH) were investigated. The results showed that Re(Hpy) and Re(Hph) are promising catalysts that have the ability to capture and convert CO_2. CV measurement of the three complexes showed two reduction waves, but the CO_2 reduction reaction occurred only at the second reduction potential. Re(Hpy) displayed the highest catalytic activity of CO_2 reduction, which was expressed by the current density and the power density. Re(Hph) displayed the lowest CO_2 reduction activity, as suggested by its low reduction potential. Under a CO_2 atmosphere, these complexes reduced CO_2 in the presence and absence of TEOA; TEOA enhanced the CO_2 reduction efficiency. The formation of Re-TEOA was suggested to increase the efficiency of capturing and inserting CO_2. The conversion of the complex into the new species Re-TEOA and Re-DMF+ after the CV study was confirmed by the change in the UV/vis spectra. Therefore, this study suggests further investigation of these complexes in bulk electrocatalysis of CO_2 conversion to analyze the formed products and quantify the concentration of the corresponding products.

4. EXPERIMENTAL SECTION

Pentacarbonylchlororhenium(I) ($[Re(CO)_5Cl]$), 2,2′-bipyridine-4,4′ dicarboxylic acid, hydrazine hydrate, 2-cyanopyridine, formic acid, silver hexafluorophosphate, tetraethylammonium tetrafluoroborate (Et_4NBF_4), and anhydrous *N*,*N*-dimethylformamide (DMF) were purchased from the Sigma Aldrich company. Triethanolamine (TEOA—$(HOCH_2CH_2)_3N$), toluene, dichloromethane, diethyl ether, and hexane solvents were of HPLC grade and were obtained from Merck and Fisher companies. All solvents and other reagents were used without further purification. Argon and carbon dioxide gases used in all experiments were of 99.99% purity.

All electrochemical measurements were performed using Bio-Logic VSP-300 and a three-electrode configuration with a scan rate of 200 mV/s. Electrochemical studies were carried out in an electrochemical cell containing 5 mL of a sample solution with a platinum (2 mm diameter) electrode, a nickel mesh electrode, and an Ag/Ag^+ electrode as the working, counter, and reference electrodes, respectively. The Ag/Ag^+ electrode was an Ag wire immersed in DMF solution containing 0.01 $AgPF_6$ and 0.1 M Et_4NBF_4, and Vycor glass was used to separate the electrode solution from the electrolyte solution. The sample solution was prepared by adding a 1 mM complex sample in DMF or DMF:TEOA (v/v 5:1 ratio)

https://doi.org/10.1021/acsomega.2c03278
ACS Omega 2022, 7, 34089−34097

containing 0.1 M Et_4NBF_4 as a supporting electrolyte. The blank DMF and DMF:TEOA solutions (containing 0.1 M Et_4NBF_4) were measured in Ar and CO_2 media. The current density (mA/cm^2) was calculated based on the surface area of the working electrode (Pt: 2 mm diameter).

Chronoamperometry measurements were performed to determine the current and the stability of the complexes in CO_2 reduction with respect to the applied voltage. The experiment was carried out for 300 s in 5 mL of the sample solution (prepared as in the electrochemical experiment) saturated with Ar or CO_2 media vs Ag/Ag^+. The applied voltage corresponding to each complex was determined on the reduction peaks obtained on the cyclic voltammograms. The powder current density was calculated using the formula $P = U \times I$ (mW/cm^2), where U (V) is the applied voltage and I (mA/cm^2) is the corresponding current density determined from the CA measurement.

A UV−vis SHIMADZU UV-1800 instrument was used to obtain the UV/vis absorption data in the transmission mode. UV/vis measurements, which were obtained before and after CV measurements, were applied to the solution containing the complex and 0.1 M Et_4NBF_4 in the DMF:TEOA mixed solvent saturated in CO_2 gas. The difference in optical density (ΔOD) is the difference between the UV/vis absorption measured after CV measurement and that measured before CV measurement.

4.1. Synthesis of Ligands 3-(2-pyridyl)-1,2,4-triazole (Hpy) and 3-(Pyridin-2-yl)-5-phenyl-l,2,4-triazole (Hph). The ligands 3-(2-pyridyl)-1,2,4-triazole and 3-(pyridin-2-yl)-5-phenyl-l,2,4-triazole were synthesized as follows.[19,28,31−33] Hydrazine hydrate (0.15 mol) was added to a mixture of 0.15 mol of 2-cyanopyridine and 40 mL of ethanol to obtain a clear solution. The clear solution was stirred at 400C until it turned into a pale-yellow solution and continuously stirred overnight at room temperature. The solution was placed at room temperature for a few days and needle-like crystals were formed. The crystals were filtered and washed with cold ethanol.

4.2. Ligand Hpy ($C_7H_6N_4$). The obtained crystal (10 g) was added to 50 mL of ice-cold formic acid. The mixture was stirred for 30 min, then brought to room temperature, and stirred for 4 h, and the excess formic acid was removed on a rotary evaporator. Then, the remaining oil was refluxed in ethylene glycol for 1 h, and after a few hours of cooling down, the precipitate was formed. The Hpy ligand was recrystallized twice from acetone to yield a fine powder. Yield: 4.15 g (41.5%). 1H NMR (500 MHz, d_6—acetone, ppm) δ = 8.67 (1H, d), 8.17 (1H, s), 8.13 (1H, s), 7.97 (1H, t), 7.47 (1H, t).

4.3. Ligand Hph ($C_{13}H_{10}N_4$). The obtained crystal (14 g) was added to the mixed solution of 10 mL of triethylamine and 30 mL of dry THF. Next, benzoyl chloride (14.1 g, 0.1 mol) was added dropwise while stirring the mixture. The dark-yellow suspension was stirred for 5 h at room temperature. The precipitate was filtered and left to dry overnight. The obtained powder was dissolved in 20 mL of ethylene glycol and refluxed for 6 h. The ethylene glycol was placed to cool to room temperature, and then, 10 mL of distilled water was added into the solution to obtain the precipitate. The ligand precipitated for several days and was then filtered. The ligand was recrystallized twice from ethanol to yield a fine powder. Yield: 5 g (17.8%). 1H NMR (400 MHz, d_6—acetone, ppm) δ = 8.70 (1H, d), 8.27 (1H, d), 8.21 (1H, m), 8.03 (1H, m), 7.52 (1H, m), 7.45 (2H, m).

4.4. Synthetic Procedure for [$Re(CO)_3Cl$(*N-N*)] Complexes. [$Re(CO)_5Cl$] (200 mg, 0.55 mM) and an appropriate ligand (0.55 mM) in 50 mL of toluene were refluxed for 6 h under an Ar atmosphere to yield a red-orange solution ([$Re(CO)_3Cl$(2,2′-bipyridine-4,4′ dicarboxylic acid)]—Re(COOH)), a yellowish solution ([$Re(CO)_3Cl$(3-(2-pyridyl)-1,2,4-triazole)]—Re(Hpy)), and a yellowish-green solution ([$Re(CO)_3Cl$(3-(pyridin-2-yl)-5-phenyl-l,2,4-triazole)]—Re(Hph)). The crude products of Re(COOH), Re(Hpy), and Re(Hph) were recrystallized from acetone−hexane, acetonitrile−hexane, and dichloromethane−hexane, respectively.

4.5. [$Re(CO)_3Cl$(2,2′-bipyridine-4,4′ dicarboxylic acid)] ($C_{15}H_8ClN_2O_7Re$). Yield: 65%. 1H NMR (500 MHz, d_6—acetone, ppm) δ = 9.33 (2H, d, bpy H6, H6′), 9.18 (2H, s, H3, H3′), 8.24−8.26 (2H, m, H5, H5′). ESI-MS (in MeCN): m/z: (M^+ for $[C_{15}H_8N_2O_7Re]^+$), 512.9 (M^{3+} for $[C_{15}H_6N_2O_7Re]^+$). $\nu_{CO/}cm^{-1}$ (in MeCN): 2041, 1956, 1897.

4.6. [$Re(CO)_3Cl$(3-(2-pyridyl)-1,2,4-triazole)] ($C_{10}H_6ClN_4O_3Re$). Yield: 44%. 1H NMR (500 MHz, d_6—acetone, ppm δ = 9.40 (1H, s, H_a), 9.05−9.07 (1H, m, H_6), 8.37−8.40 (1H, m, H_3), 8.31−8.35 (1H, m, H_4), 7.77−7.80 (1H, m, H_5)). ESI-MS (in MeCN): m/z: 450.69 (M^+ for $[Re(C_7H_5N_4)(CO)_3Cl]^+$), 448.73 ($M^{3+}$ for $[Re(C_7H_3N_4)(CO)_3Cl]^{3+}$), 422.71 (for $[Re(C_7H_5N_4)(CO)_2Cl]^{2+}$). $\nu_{CO/}cm^{-1}$ (in MeCN): 2027, 1915, 1890.

4.7. [$Re(CO)_3Cl$(3-(pyridin-2-yl)-5-phenyl-l,2,4-triazole)] ($C_{16}H_{10}ClN_4O_3Re$). Yield: 56%. 1H NMR (500 MHz, d_6—acetone, ppm) δ = 9.09 (1H, d, H6), 8.46 (1H, d, H3), 8.36−8.39 (1H, m, H4), 8.19 (2H, m, Ha), 7.80−7.82 (1H, m, H5), 7.64 (2H, d, Hb), 7.62 (1H, m, Hc). ESI-MS (in MeCN): m/z: 493.03 (M^+ for $[Re(C_{13}H_{10}N_4)(CO)_3]^+$), 465 ($M^+$ − CO), 534 (M^+ + MeCN). $\nu_{CO/cm}{}^{-1}$ (in MeCN): 2025, 1923, 1894.

■ ASSOCIATED CONTENT

Supporting Information

The Supporting Information is available free of charge at https://pubs.acs.org/doi/10.1021/acsomega.2c03278.

Proton nuclear magnetic resonance spectroscopy (^1H NMR) of Hpy and Hph ligands; electrospray ionization mass spectroscopy (ESI-MS); FTIR spectra; and difference in optical densities between UV/vis spectra obtained before CV measurements and that in MeCN solution of Re(Hpy), Re(Hph), and Re(COOH) (PDF)

■ AUTHOR INFORMATION

Corresponding Author

Tuan M. Nguyen − *Institute of Applied Materials Science, Vietnam Academy of Science and Technology (VAST), Ho Chi Minh City 700000, Vietnam; Graduate University of Science and Technology, VAST, Ha Noi 100000, Vietnam;* orcid.org/0000-0003-0678-1058; Email: nguyenmanhtuan@iams.vast.vn

Authors

Phuong N. Nguyen − *Institute of Applied Materials Science, Vietnam Academy of Science and Technology (VAST), Ho Chi Minh City 700000, Vietnam; Graduate University of Science and Technology, VAST, Ha Noi 100000, Vietnam;* orcid.org/0000-0003-0302-7455

Thi-Bich-Ngoc Dao − *Future Materials & Devices Lab., Institute of Fundamental and Applied Sciences, Duy Tan*

https://doi.org/10.1021/acsomega.2c03278
ACS Omega 2022, 7, 34089−34097

University, Ho Chi Minh City 700000, Vietnam; The Faculty of Environmental and Chemical Engineering, Duy Tan University, Danang 550000, Vietnam; orcid.org/0000-0002-1410-3727

Trang T. Tran − *Institute of Applied Materials Science, Vietnam Academy of Science and Technology (VAST), Ho Chi Minh City 700000, Vietnam; Department Materials Science and Technology, University of Science, Ho Chi Minh City 700000, Vietnam*

Ngoc-Anh T. Tran − *Institute of Applied Materials Science, Vietnam Academy of Science and Technology (VAST), Ho Chi Minh City 700000, Vietnam; Department Materials Science and Technology, University of Science, Ho Chi Minh City 700000, Vietnam*

Tu A. Nguyen − *Institute of Applied Materials Science, Vietnam Academy of Science and Technology (VAST), Ho Chi Minh City 700000, Vietnam; Department Materials Science and Technology, University of Science, Ho Chi Minh City 700000, Vietnam*

Thao-Dang L. Phan − *Institute of Applied Materials Science, Vietnam Academy of Science and Technology (VAST), Ho Chi Minh City 700000, Vietnam; Department Materials Science and Technology, University of Science, Ho Chi Minh City 700000, Vietnam*

Loc P. Nguyen − *Institute of Applied Materials Science, Vietnam Academy of Science and Technology (VAST), Ho Chi Minh City 700000, Vietnam; Department Materials Science and Technology, University of Science, Ho Chi Minh City 700000, Vietnam*

Vinh Q. Dang − *Department Materials Science and Technology, University of Science, Ho Chi Minh City 700000, Vietnam; Vietnam National University, Ho Chi Minh (VNU-HCM), Ho Chi Minh City, Vietnam*

Nam N. Dang − *Future Materials & Devices Lab., Institute of Fundamental and Applied Sciences, Duy Tan University, Ho Chi Minh City 700000, Vietnam; The Faculty of Environmental and Chemical Engineering, Duy Tan University, Danang 550000, Vietnam*

Complete contact information is available at: https://pubs.acs.org/10.1021/acsomega.2c03278

Author Contributions

P.N.N. designed the experiments, analyzed data, and wrote the text. T.T.T., N.-A.T.T., and L.P.N. obtained CV and UV/vis data. T.A.N., T.-D.L.P., V.Q.D., and T.-B.-N.D. synthesized materials and analyzed their structures. T.M.N. supervised the project and corrections. N.N.D. partly designed the project and corrections. All authors contributed to data analysis and approved the final version of the manuscript.

Notes

The authors declare no competing financial interest.

■ ACKNOWLEDGMENTS

The authors are very grateful for financial support from the Vietnam Academy of Science and Technology under Grant Number VAST03−07/21-22.

■ REFERENCES

(1) https://www.eia.gov/outlooks/steo/ April 7, 2022.

(2) Birdja, Y. Y.; Pérez-Gallent, E.; Figueiredo, M. C.; Göttle, J. A.; Calle-Vallejo, F.; Koper, T. M. M. Advances and challenges in understanding the electrocatalytic conversion of carbon dioxide to fuels. *Nat. Energy* **2019**, *4*, 732−745.

(3) Ansari, K. B.; Gaikar, V. G.; Trinh, Q. T.; Khan, M. S.; Banerjee, A.; Kanchan, D. A.; Al Mesfer, M. K.; Danis, M. Carbon dioxide capture over amine functionalized styrene divinylbenzene copolymer: An experimental batch and continuous studies. *J. Environ. Chem. Eng.* **2022**, *10*, No. 106910.

(4) Liu, G.; Narangari, P. R.; Trinh, Q. T.; Tu, W.; Kraft, M.; Tan, H. H.; Jagadish, C.; Choksi, T. S.; Ager, J. W.; Karuturi, S.; Xu, R. Manipulating Intermediates at the Au−TiO_2 Interface over InP Nanopillar Array for Photoelectrochemical CO_2 Reduction. *ACS Catal.* **2021**, *11*, 11416−11428.

(5) Wu, J.; Huang, Y.; Ye, W.; Li, Y. CO_2 Reduction: From the Electrochemical to Photochemical Approach. *Adv. Sci.* **2017**, *4*, No. 1700194.

(6) Melis, N.; Mocci, F.; Vacca, A.; Pilia, L. Novel homogeneous selective electrocatalysts for CO_2 reduction: an electrochemical and computational study of cyclopentadienyl-phenylendiamino-cobalt complexes. *Sustainable Energy Fuels* **2020**, *4*, 5609−5617.

(7) Zeng, J.; Fiorentin, M. R.; Fontana, M.; Castellino, M.; Risplendi, F.; Sacco, A.; Cicero, G.; Farkhondehfal, M. A.; Drago, F.; Pirri, C. F. Novel insights into Sb-Cu catalysts for electrochemical reduction of CO_2. *Appl. Catal., B* **2022**, *306*, No. 121089.

(8) Talukdar, K.; Roy, S. S.; Amatya, E.; Sleeper, E. A.; Magueres, P. L.; Jurss, J. W. Enhanced electrochemical CO_2 reduction by a series of molecular Rhenium catalysts decorated with second-sphere hydrogen-bond donors. *Inorg. Chem.* **2020**, *59*, 6087−6099.

(9) Smieja, J. M.; Kubiak, C. P. Re(bipy-tBu)$(CO)_3$Cl-improved catalytic activity for reduction of carbon dioxide: IR-spectroelectrochemical and mechanistic studies. *Inorg. Chem.* **2010**, *49*, 9283−9289.

(10) Kumagai, H.; Nishikawa, T.; Koizumi, H.; Yatsu, T.; Sahara, G.; Yamazaki, Y.; Tamakia, Y.; Ishitani, O. Electrocatalytic reduction of low concentration CO_2. *Chem. Sci.* **2019**, *10*, 1597−1606.

(11) Nakada, A.; Ishitani, O. Selective Electrocatalysis of a Water-Soluble Rhenium(I) Complex for CO_2 Reduction Using Water As an Electron Donor. *ACS Catal.* **2018**, *8*, 354−363.

(12) Sampson, M. D.; Nguyen, A. D.; Grice, K. A.; Moore, C. E.; Rheingold, A. L.; Kubiak, C. P. Manganese catalysts with bulky bipyridine ligands for the electrocatalytic reduction of carbon dioxide: Eliminating dimerization and altering catalysis. *J. Am. Chem. Soc.* **2014**, *136*, 5460−5471.

(13) Koizumi, H.; Chibaa, H.; Sugiharab, A.; Iwamurab, M.; Nozaki, K.; Ishitani, O. CO_2 capture by Mn(i) and Re(i) complexes with a deprotonated triethanolamine ligand. *Chem. Sci.* **2019**, *10*, 3080−3088.

(14) Taylor, J. O.; Neri, G.; Banerji, L.; Cowan, A. J.; Hartl, F. Strong impact of intramolecular hydrogen bonding on the cathodic path of [Re(3,3′-dihydroxy-2,2′-bipyridine)$(CO)_3$Cl] and catalytic reduction of carbon dioxide. *Inorg. Chem.* **2020**, *59*, 5564−5578.

(15) Grice, K. A.; Saucedo, C. Electrocatalytic reduction of CO_2 by group 6 $M(CO)_6$ species without "non-innocent" ligands. *Inorg. Chem.* **2016**, *55*, 6240−6246.

(16) Costentin, C.; Drouet, S.; Robert, M.; Savéant, J. M. A local proton source enhances CO_2 electroreduction to CO by a molecular Fe catalyst. *Science* **2012**, *338*, 90−94.

(17) Stanton, C. J.; Machan, C. W.; Vandezande, J. E.; Jin, T.; Majetich, G. F.; Schaefer, H. F.; Kubiak, C. P.; Li, G.; Agarwal, J. Re(I) NHC complexes for electrocatalytic conversion of CO_2. *Inorg. Chem.* **2016**, *55*, 3136−3144.

(18) Liyanage, N. P.; Dulaney, H. A.; Huckaba, A. J.; Jurss, J. W.; Delcamp, J. H. Electrocatalytic reduction of CO_2 to CO with Re-pyridyl-NHCs: Proton source influence on rates and product selectivities. *Inorg. Chem.* **2016**, *55*, 6085−6094.

(19) Burke, H. M.; Gallagher, J. F.; Indelli, M. T.; Vos, J. G. The synthesis and characterisation of Rh(III) complexes with pyridyl triazole ligands. *Inorg. Chim. Acta* **2004**, *357*, 2989−3000.

(20) Felici, M.; Contreras-Carballada, P.; Vida, Y.; Smits, J. M. M.; Nolte, R. J. M.; Cola, L. D.; Williams, R. M.; Feiters, M. C. IrIII and

RuII complexes containing triazole-pyridine ligands: Luminescence enhancement upon substitution with β-cyclodextrin. *Chem. − Eur. J.* **2009**, *15*, 13124−13134.
(21) Browne, W. R.; O'Connor, C. M.; Hughes, H. P.; Hage, R.; Walter, O.; Doering, M.; Gallagher, J. F.; Vos, J. G. Ruthenium(II) and osmium(II) polypyridyl complexes of an asymmetric pyrazinyl- and pyridinyl-containing 1,2,4-triazole based ligand. Connectivity and physical properties of mononuclear complexes. *J. Chem. Soc., Dalton Trans.* **2002**, 4048−4054.
(22) Adhikari, S.; Sutradhar, D.; Shepherd, S. L.; Phillips, R. M.; Chandra, A. K.; Rao, K. M. Synthesis, structural, DFT calculations and biological studies of rhodium and iridium complexes containing azine Schiff-base ligands. *Polyhedron* **2016**, *117*, 404−414.
(23) Weldon, F.; Hammarstrom, L.; Mukhtar, E.; Hage, R.; Gunneweg, E.; Haasnoot, J. G.; Reedijk, J.; Browne, W. R.; Guckian, A. L.; Vos, J. G. Energy transfer pathways in dinuclear heteroleptic polypyridyl complexes: Through-space vs through-bond interaction mechanisms. *Inorg. Chem.* **2004**, *43*, 4471−4481.
(24) Gerschel, P.; Cordes, A. L.; Bimmermann, S.; Siegmund, D.; Metzler-Nolte, N.; Apfel, U.-P. Investigation of cyclam based Re-Complexes as potential electrocatalysts for the CO_2 reduction reaction. *Z. Anorg. Allg. Chem.* **2021**, *647*, 968−977.
(25) Haasnoot, J. G. Mononuclear, oligonuclear and polynuclear metal coordination compounds with 1,2,4-triazole derivatives as ligands. *Coord. Chem. Rev.* **2000**, *200-202*, 131−185.
(26) Klingele, M. H.; Brooker, S. The coordination chemistry of 4-substituted 3,5-di(2-pyridyl)-4H-1,2,4-triazoles and related ligands. *Coord. Chem. Rev.* **2003**, *241*, 119−132.
(27) Ching, H. Y. V.; Wang, X.; He, M.; Holland, N. P.; Guillot, R.; Slim, C.; Griveau, S.; Bertrand, H. C.; Policar, C.; Bedioui, F.; Fontecave, M. Rhenium complexes based on 2-Pyridyl-1,2,3-triazole ligands: A new class of CO_2 reduction catalysts. *Inorg. Chem.* **2017**, *56*, 2966−2976.
(28) Obata, M.; Kitamura, A.; Mori, A.; Kameyama, C.; Czaplewska, J. A.; Tanaka, R.; Kinoshita, I.; Kusumoto, T.; Hashimoto, H.; Harada, M.; Mikata, Y.; Funabiki, T.; Yano, S. Syntheses, structural characterization and photophysical properties of 4-(2-pyridyl)-1,2,3-triazole rhenium(i) complexes. *Dalton Trans.* **2008**, *25*, 3292−3300.
(29) Aimene, Y.; Eychenne, R.; Mallet-Ladeira, S.; Saffon, N.; Winum, J-Y.; Nocentini, A.; Supuran, C.; Benoist, E.; Seridi, A. Novel Re(I) tricarbonyl coordination compounds based on 2-pyridyl-1,2,3-triazole derivatives bearing a 4-amino-substituted benzenesulfonamide arm: synthesis, crystal structure, computational studies and inhibitory activity against carbonic anhydrase I, II. *J. Enzyme Inhib. Med. Chem.* **2019**, *34*, 773−782.
(30) Bertrand, H. C.; Clède, S.; Guillot, R.; Lambert, F.; Policar, C. Luminescence modulations of rhenium tricarbonyl complexes induced by structural variations. *Inorg. Chem.* **2014**, *53*, 6204−6223.
(31) Liu, H.; Sun, L.; Zhou, H.; Cen, P.; Jin, X.; Lui, X.; Hu, Q. A mononuclear cobalt(III) 3-(2-pyridyl)-5-phenyl-1,2,4-triazolato complex: Hydrothermal synthesis, crystal structure, thermostability, and DFT calculations. *Z. Naturforsch. B* **2015**, *70*, 631−636.
(32) Bolje, A.; Urankar, D.; Košmrlj, J. Synthesis and NMR analysis of 1,4-disubstituted 1,2,3-triazoles tethered to pyridine, pyrimidine, and pyrazine rings. *Eur. J. Org. Chem.* **2014**, *2014*, 8167−8181.
(33) Cheng, L.; Zhang, W.-X.; Ye, B.-H.; Lin, J.-B.; Chen, X.-M. In situ solvothermal generation of 1,2,4-triazolates and related compounds from organonitrile and hydrazine hydrate: A mechanism study. *Inorg. Chem.* **2007**, *46*, 1135−1143.
(34) Brennan, C. Synthesis and Characterisation of Mononuclear and Dinuclear Rhenium Carbonyl. Ph.D. Thesis, Dublin City University, 2007.
(35) Morimoto, T.; Nakajima, T.; Sawa, S.; Nakanishi, R.; Imori, D.; Ishitani, O. CO_2 capture by a rhenium(I) complex with the aid of triethanolamine. *J. Am. Chem. Soc.* **2013**, *135*, 16825−16828.
(36) Nganga, J. K.; Samanamu, C. R.; Tanski, J. M.; Pacheco, C.; Saucedo, C.; Batista, V. S.; Grice, K. A.; Ertem, M. Z.; Angeles-Boza, A. M. Electrochemical reduction of CO_2 catalyzed by re(pyridine-oxazoline)$(CO)_3$Cl complexes. *Inorg. Chem.* **2017**, *56*, 3214−3226.
(37) Yamazaki, Y.; Takeda, H.; Ishitani, O. Photocatalytic reduction of CO_2 using metal complexes. *J. Photochem. Photobiol., C* **2015**, *25*, 106−137.
(38) Mukherjee, J.; Siewert, I. Manganese and Rhenium tricarbonyl complexes equipped with proton relays in the electrochemical CO_2 reduction reaction. *Eur. J. Inorg. Chem.* **2020**, *2020*, 4319−4333.
(39) Hayashi, Y.; Kita, S.; Brunschwig, B. S.; Fujita, E. Involvement of a binuclear species with the Re−C(O)O−Re moiety in CO_2 reduction catalyzed by tricarbonyl rhenium(I) complexes with diimine ligands: Strikingly slow formation of the Re−Re and Re−C(O)O−Re species from Re(dmb)$(CO)_3$S (dmb = 4,4'-Dimethyl-2,2'-bipyridine, S = Solvent). *J. Am. Chem. Soc.* **2003**, *125*, 11976−11987.

https://doi.org/10.1021/acsomega.2c03278
ACS Omega 2022, 7, 34089−34097